Shadow monochromatic backlighting: Large-field high resolution X-ray shadowgraphy with improved spectral tunability

T. A. Pikuz[a], A. Ya. Faenov[a] , M. Fraenkel[b1], A. Zigler[b], F. Flora[c], S.Bollanti[c], P.Di Lazzaro[c], T. Letardi[c], A. Grilli[d], L.Palladino[e], G. Tomassetti[e], A. Reale[e], L. Reale[e], A. Scafati[e], T. Limongi[e], F. Bonfigli[f], L.Alainelli[g], M.Sanchez del Rio[g]

[a] Multicharged Ions Spectra Data Center of VNIIFRTI, Mendeleevo, Moscow Region, 141570, Russia
[b] Racah Institute of Physics, The Hebrew University of Jerusalem, Jerusalem 91904, Israel
[c] ENEA, Dipartimento Innovazione, Settore Fisica Applicata, 00044 Frascati, Italy
[d] INFN Frascati, 00044 Frascati, Italy
[e] INFM Dipartamento di Fisica dell'Aquila and LNGS-INFN, Assergi (L'Aquila), Italy
[f] EL.EN. S.p.A., Calenzano (FI), Italy
[g]European Synchrotron Radiation Facility, BP 220, F-38043 Grenoble Cedex, France

Abstract

The Shadow Monochromatic Backlighting (SMB) scheme, a modification of the well-known soft X-ray monochromatic backlighting scheme, is proposed. It is based on a spherical crystal as the dispersive element and extends the traditional scheme by allowing working with a wide range of Bragg angles and therefore with a wide spectral range. The advantages of the new scheme are demonstrated experimentally and supported numerically by ray-tracing simulations. In the experiments, the X-ray backlighter source is a laser-produced plasma, created by the interaction of ultra short pulse, Ti:Sapphire laser (120 fs, 3-5 mJ, 10^{16} W/cm^2 on target) or short wavelength XeCl laser (10 ns, 1-2 J, 10^{13} W/cm^2 on target) with various solid targets (Dy, Ni+Cr, BaF_2). In both experiments, the X-ray sources are well localized both spatially (~20 μm) and are spectrally tunable in a relatively wide wavelengths range (λ=8-15 Å). High quality monochromatic ($\delta\lambda/\lambda$~10^{-5}-10^{-3}) images with high spatial resolution (up to ~4 μm) over a large field of view (few mm^2) were obtained. Utilization of the spherically bent crystals for obtaining high-resolution, large field, monochromatic images in a wide range of Bragg angles ($35°<\Theta<90°$) is demonstrated for the first time.

---

[1] Current address: Plasma Physics Department, Soreq NRC, Yavne 81800, Israel.

I. Introduction

During the last 20 years, X-ray radiography techniques have been successfully used as a method of dense plasma diagnostics in experiments such as inertial confinement fusion, X-ray laser, high current pinch discharges and high-energy density physics. Nowadays, monochromatic backlighting schemes (see, for example, Miyanaga et al. 1983, Balmer et al.1989, Perry et al.1991, Edwards et al. 1991, Back et al. 1992) and X-ray lasers (Da Silva et al. 1995, Cauble et al. 1995) are widely used for these purposes. Recently, a spherically bent crystal was utilized as the X-ray dispersive element (Belyaev et al. 1976, Rode et al. 1990, Pikuz S. et al. 1995,1997, Pikuz T. et al. 1995, Marshall and Su 1995, Aglitskiy et al. 1996,1997,1998,1999, Brown et al. 1997, Sancez del Rio et al. 1997, Anfelo et al. 1998, Koch et al. 1998, 1999, Fraenkel et al. 1999a, Workman et al. 1999, Missala et al. 1999). Monochromatic images with spatial resolution of up to 1.7 μm in a field of view of 1 mm^2 (Aglitskiy et al. 1998), and spatial resolution of about 4 μm in a field of view of about 10 mm^2 (Pikuz S. et al. 1997) have been experimentally demonstrated using these crystals. Advantages of the spherically bent crystals include: high luminosity due to the focusing feature of the spherical surface, the possibility to distinguish between the backlighter monochromatic radiation and the object plasma radiation by proper shielding, and more. Nevertheless, the high spatial resolution can be obtained in this scheme only when the radiation angle of incidence on the crystal surface is close to normal (usually 80^o-88^o). This limits the spectral range that can be used for imaging, to values close to 2*d* of the crystal. Due to the limited variety of crystals that

can be spherically bent with high quality, the wavelength selection ability for the monochromatic backlighting technique is severely limited.

In this paper we propose utilization of the spherical crystals in a modified X-Ray backlighting scheme, which allows operation with practically any Bragg angle (thus, with a wide spectral range), while keeping high spatial resolution in a large field of view. The Shadow Monochromatic Backlitighting (SMB) scheme (the name was chosen due to its similarity to the shadow geometry imaging scheme) provides also the possibility to image 3D objects with high spatial resolution.

II. Description and ray-tracing modeling of the SMB scheme

As was described above, the SMB scheme is a modification of the successfully used monochromatic X-Ray backlighting approach, based on spherically bent crystal as the dispersive element. For better understanding of the main differences between these two approaches, both schemes are shown in Fig1a,b. In both schemes the spherical crystal is mounted on the Rowland circle (the circle whose diameter equals the spherical crystal radius of curvature, R). The backlighter source is also placed on the Rowland circle, at the distance s from the crystal. Due to Bragg diffraction conditions, only monochromatic light ($\delta\lambda/\lambda \sim 10^{-5}$-$10^{-3}$) is reflects by the crystal (Fraenkel et. al. 1997, Hölzer et. al. 1998).

In the usual monochromatic X-ray backlighter scheme (Fig. 1a), the investigated object is placed between the source and the crystal at the distance a from the crystal, and the monochromatic image is detected at a distance $b = Ra/(2a \sin\Theta - R)$ from the crystal.

The distance b is determined according to the usual optical equation $1/a+1/b = 2\sin\Theta / R$, and the magnification is $M = b / a$.

In this X-Ray backlighting monochromatic scheme, we must restrict ourselves to Bragg angles in the limited range of about 80°÷88°, since working with smaller angels introduces severe astigmatism to the image, which limits the possibility to obtain high spatial resolution (Sancez del Rio et al. 1997). These in turn limits the imaging possibilities to a narrow spectral range, close to the crystal interplanar spacing $2d$. Moreover, if large magnification is desired, the crystal-detector distance b must be increased. This leads to intensity losses and also introduces additional technical problems (large vacuum chamber is needed and complicated alignment is required).

The astigmatism mentioned above originates from the fact that when highly off-axis configuration is used, the beam reflected by the crystal is not symmetrical. Two waists appear: one at the position of the tangential focus F_t, and the other at the position of the sagittal focus F_s (see Fig. 1b). On the contrary, it can be easily shown by geometrical considerations (Fig. 1b), that for any Bragg angle, specific positions for the object and detector can be found, for which the image will have the same width (in the tangential - or diffraction - axis) and height (in the sagittal axis) as the object, and thus similar shape as the object. For example, for a spherical crystal with a square working area, these object-image positions are defined as

$$p_0 = q = (f_t^2 - f_t f_s) / (f_t + f_s), \qquad (1)$$

where p_0 is the source-object distance, q is the distance from tangential focus to the image plane; $f_t = R\sin\Theta$ and $f_s = R\sin\Theta / \cos 2\Theta$ are the tangential and sagittal foci of the spherical crystal, respectively (for a given Bragg angle Θ and crystal radius of curvature

R). As can be seen from eq. 1 and Fig. 1a, for Θ close to 90°, the focal planes F_t and F_s practically coincide. Therefore, it is clear, that if the object is placed at a distance p_0 from the source, we can observe its image at a distance q from the tangential focus with a unit magnification. This means that the image is stigmatic and not deformed, despite the large angle of incidence to the surface of spherically bent crystal.

If the position of the image plane (and thus the image size) is fixed, than the magnification can be changed by moving the object along the source – crystal direction. If $p_i > p_0$ the magnification is $M < 1$ (Fig. 1b), and if $p_i < p_0$ the magnification is $M > 1$. Numerically, the magnification is $M = q / p_i$, where p_i is the object position (and $q=p_0$).

For the simulation of the SMB scheme, the SHADOW ray-tracing package was used (Sancez del Rio et al. 1995, 1997,1999). This package is capable of dealing with wide range of problems related to the X-Ray backlighting modeling field, including strongly off-axis and asymmetric optics, special diffractive optics as crystals, and special source geometry like laser-produced plasma with different sizes or other plasma sources. SHADOW creates a fan of rays in a given region of the space (source). A ray is a point in a multidimensional space, which contains the starting point coordinates, the direction vector, the photon energy and other parameters describing, for example, the ray intensity, a label, ray-flag, etc. The rays emitted by the source are created using the Monte Carlo technique to sample the spatial, angular and spectral distribution. This allows us to simulate different types of sources such as: point source, rectangular, circular etc. The angular distribution is selected out of a number of options, which include flat, uniform, Gaussian, etc.

In the following simulations we used an ideal point source, which creates a spherical wave front. The mica crystal reflectivity has not been taken into account for the calculations. In other words, we have considered the crystal as a mirror-like system, therefore only the geometrical study has been performed. This approximation is good enough for spatial resolution calculations when using almost perfect crystals in Bragg geometry, as in our case of high quality mica crystals. The point X-Ray backlighter source was placed on the Rowland circle. A mica crystal with radius of curvature R = 104.3 mm was mounted at a distance s = 88 mm from the source and was illuminated at Bragg angle of Θ=57.5° with source divergence of 40 mrad. The investigated object was a test grid (120 μm period and 14 μm wires thickness). Two geometrical configurations were modeled, for different positions of the grid: p_1 = 38 mm (M = 0.94 - small demagnification) and p_2 = 8.8 mm (M = 4.05). Very sharp, anastigmatic images with good aspect ratio were obtained for both cases (see Fig 2a and 2b for the distances p_1 and p_2, respectively). The ray-tracing modeling thus clearly demonstrates the possibility to obtain highly resolved images using the SMB scheme with Bragg angles far from normal.

III. SMB scheme experimental demonstration

Laser produced plasma, generated by the interaction of intense femtosecond Ti:Sapphire or ns excimer laser pulses with a solid target, was used as a X-ray backlighter source for our test experiments. In the first series of experiments, the table-top Ti:Sapphire laser (previously described by Fraenkel et al. 1997) was used to create the

plasma. It has pulse duration of 120 fs, energy of 3-5 mJ per pulse and a repetition rate of 10 Hz. The laser pulses are focused on a solid target to a focal spot of ~20 μm in diameter (Faenov et al. 1997) to produce power density of 10^{16} W/cm^2. The plasma formed has electron density in the order of (0.5-1.0)x10^{22} cm^{-3}, electron temperature in the range of 100-200 eV and it emits intense short bursts of X-rays (Doron et al. 1998, Fraenkel et al. 1999a,b). In the second series of experiments a large-volume XeCl excimer laser Hercules (Bollanti et al. 1996,1998) was used as a laser source. The laser has energy of 1-1.3 J per pulse, repetition rate of up to 10 Hz, pulse duration of 10 ns and the power density on target was about 10^{13} W/cm^2. The plasma formed has again electron density of around (0.5-1.0)x10^{22} cm^{-3} and electron temperature between 50 and 400 eV (Rosmej et al. 1997, Stepanov et al. 1997).

In our experiments we have used mica spherically bent crystals ($2d \approx 19.9$ Å) with radius of curvature R=100 mm and R=80 mm and aperture sizes of 10 mm x 30 mm. The crystals were used in the first or second orders of reflection. By choosing the proper target material and laser intensity, we been able to create an intense soft X-ray radiation in the desired X-ray spectral range. The most efficient lines for monochromatic backlighting, are the intense resonance lines of ions of different elements. In our case we have used emission of resonance lines of Ne-like Ni and of Ni-like ions of Ba and Dy. Solid BaF_2, Dy and Ni+Cr were used as targets. Different grids and grids combinations were used as test-objects. In all experiments, the images were detected on the a Kodak X-ray DEF film. It was necessary to expose the film to around 300 shots of XeCl laser and around 10,000 shots (about 20 minutes of exposure) of Ti:Sapphire laser to collect appropriate intensity for high contrast images.

The backlighter source in the Ti:Sapphire laser experiments was created by the laser pulse interaction with BaF_2 target, producing emission of Ni-like ions of Ba with wavelength λ = 13.1 Å. The source was located on the Rowland circle with R = 100 mm at the Bragg angle Θ = 41°. The image of a double grid, obtained with magnification of M = 4.2, is shown in Fig. 3. It can be clearly seen that the image is unastigmatic and has high spatial resolution over the whole field of view (about 2 mm x 2 mm). Densitogramm of the detailed part demonstrates that spatial resolution of about 8 μm was achieved. High quality images with magnification of 8.5 were also obtained using the same double grid object, and crystal in second order of reflection, for the wavelength of λ = 8.3 Å (Θ = 57.7°). In this case emission of Ni-like Dy ions was used as the backligther source.

In Figs. 4 – 6 we present results obtained with plasma X-ray source created by the interaction of XeCl laser with Ni+Cr target. Emission of Ne-like Ni ion at a wavelength of λ = 12.65 Å (Θ =39.4 °) was used to create the monochromatic image of a double grid, shown in Fig. 4. Again, very sharp image in a field of view of 1.2 mm x 2 mm can be observed. Densitogramm of the image shows, that the spatial resolution is slightly different for different directions: the FWHM of a single wire image (with 14 μm thickness in the object plane) is about 15 μm in the horizontal direction and about 18 μm in the vertical direction. But from the figure it is clearly seen that spatial resolution about 3 micron was obtained for the whole image field of view.

In the following experiment we check an important feature of the SMB scheme, which is the possibility to image not only a plane object, but also a 3D object, like plasma, biological or other structured objects with finite thickness. For this purpose, the test-object consisted of two separate similar grids (with wire thickness of 10 μm and

period of 65 μm), which were mounted 2.5 mm apart of each other along the backlighter-crystal direction, and turned by 45° relative to each other. In Fig. 5 the image, which was obtained at the wavelength of 14.1 Å ($\Theta = 45°$) is shown. It is clearly seen that both meshes are very well resolved. Therefore, the SMB scheme allows us to receive high spatial resolution of up to 3-4 μm in any part of thick objects. For a better demonstration of this important feature, a high quality image of a mosquito (actual 3D nonhomogeneous object) is shown in Fig.6. For this experiment, the same geometrical and illumination parameters as in Fig. 5 were used.

It is necessary to point out, that for all of these experiments, the X-Ray backlitgher sources were placed on the Rowland circle, very close or exactly at (2 last cases) the focal length $f = R/2$ of the crystal spherical surface. The object-crystal distances were smaller than f, i.e. in the region, where for usual optics it is impossible to have imaging. Nevertheless, using the SMB scheme, high quality images were obtained.

IV. Conclusion

It was demonstrated both experimentally and by ray-tracing modeling, that the proposed Shadow Monochromatic Backlighting (SMB) scheme allows us to extend the monochromatic backlighting spectral range, due to the possibility to operate in a wide range of Bragg angles ($35° < \Theta < 90°$ and even smaller angles). Using the currently available spherically bent crystals, it is practically possible to perform X-Ray backlighting experiments with any wavelengths in the 1-18 Å spectral range. The SMB requires X-ray source similar to the traditionally used backlighters.. The main advantage of the proposed scheme is in the simultaneous achievement of:

a) High spatial resolution, of up to 3-4 μm was achieved in our experiments;

b) The high resolution is obtained over a large filed of view of about 3-5 mm^2. Even larger fields of view can be achieved using the same technique.

c) Images of thick objects can be obtained with high spatial resolution over all object parts. In our experiments 2.5 mm object depth was demonstrated, and thicker objects can be imaged as well.

d) Very simple alignment, compared to the traditionally used X-Ray monochromatic backlighter scheme based on spherically bent crystals. Also, the experimental layout is much smaller (for the same magnification), thus a smaller experimental vacuum chamber is needed.

e) It is possible to use practically any bright line in the spectral range 1-18 Å as a monochromatic backlighter X-Ray source.

The SMB scheme can be used for the investigation of relatively large objects, like different plasmas (z-pinch, liner plasmas, laser produced plasmas, ion beam generated plasmas and plasmas in shock-wave related experiments), biological objects, and other structured objects. It may become a useful experimental tool in the near future, when plasma sized in different installation will reach 10 mm^3 or more, and the plasma homogeneity will have to be determined with superb spatial resolution.

Figure captions

Fig.1. Comparison of the monochromatic backlighting schemes, based on spherically bent crystals for the cases

One) usual scheme for Bragg angles Θ near 90°, where of object and image positions are determined by the optical equation $1/a + 1/b = 2 \sin \Theta / \boldsymbol{R}$

Two) SMB scheme for Bragg angles Θ << 90°, where the image plane is fixed at the distance $q = (f_t^2 - f_t f_s) / (f_t + f_s)$

Fig. 2. The image of a test-grid (wire thickness 14 μm, period 120 μm) using the SMB scheme with magnification of M = 0.94 (a) and M = 4.05 (b), obtained by the SHADOW ray-tracing modeling code.

Fig. 3. Monochromatic image of a double grid (thin grid: wire thickness 14 μm, period 120 μm; thick grid: wire thickness 170 μm), obtained by the SMB scheme at the wavelength 13.1 Å (Θ = 41°) with magnification M = 4.2, and densitogramm of a detail. Ti:Sapphire laser with pulse energy of 5 mJ and duration of 120 fs was used to create Ba plasma on a BaF_2 target. Mica crystal with radius of curvature R = 100 mm was used in the first order of reflection.

Fig. 4. Monochromatic image of a double grid (thin grid: wire thickness 14 μm, period 120 μm; thick grid: wire thickness 60 μm, period 760 μm), obtained by the SMB scheme at the wavelength 12.65 Å (Θ = 39.4°) with magnification M = 5, and densitogram of a detail. XeCl laser with pulse energy of 1.3 J and duration of 10 ns was used to create plasma on a Ni+Cr target. Mica crystal with radius of curvature R = 80 mm was used in the first order of reflection.

Fig. 5. Monochromatic image of two small grids with wire thickness of 10 μm and period of 65 μm obtained by the SMB scheme at the wavelength 14.1 Å (Θ = 45°) and densitogramms of the image. The grids are mounted 2.5 mm apart of each other along the

backlighter-crystal direction, and turned by 45° relative to each other. XeCl laser with pulse energy of 1.3 J and duration of 10 ns was used to create plasma on a Ni+Cr target. Mica crystal with radius of curvature R = 80 mm was used in the first order of reflection. The magnification M is about 4.

Fig. 6. Monochromatic image of a mosquito, obtained at the same conditions as in Fig.5.

REFERENCES

Aglitskiy,Y. et al. 1996 *Phys. Plasmas* **3**, 3438.

Aglitskiy,Y. et al. 1997 Rev. Sci. Instr. **68**, 805.

Aglitskiy,Y. et al. 1998 *Applied Optics* **37**, 5253.

Aglitskiy, Y. et al.1999 *Rev. Sci. Instrum*., **70**, 530.

Anfelo,P.et al. 1998 *Laser and Particle Beam***16**, 21.

Back, C.A. et al. 1992 *Phys. Rev.* **A46,** 3405

Balmer,J. et al. 1989 *Phys. Rev.* **A40**, 330.

Belyaev, L.M. et al. 1976 *Sov. J. Quantum Electron.* **6**, 1121.

Bollanti, S. et al. 1996 *Il Nuovo Cimento* **18D**, 1241.

Bollanti, S. et al. 1998 *Il Nuovo Cimento* **20D**, 1685.

Brown, C. et al. 1997 *Rev. Sci. Instrum*. **68**, 1099.

Cauble, R. et al. 1995 *Phys. Rev. Lett.* **74**, 3816.

Da Silva, L.B. et al. 1995 *Rev. Sci. Instrum.* **66**, 574.

Doron, R. et al.1998 Phys. Rev.A. **58**, 1859.

Edwards, J. et al. 1991 *Phys. Rev. Lett.* **67**, 3780.

Faenov, A.Ya. et al.1997 *Physica Scripta* **55**, 167.

Fraenkel, M. et al. 1997 *Physica Scripta* **56,** 571.

Fraenkel, M. et al. 1999a *Physica Scripta* **59**, 246.

Fraenkel, M. et al. 1999b *Physica Scripta* **60**, 222.

Hölzer, G. et. al. 1998 Physica Scripta **57**, 301.

Koch, J.A. et al. 1998 *Applied Optics* **37**, 1784.

Koch, J.A. et al. 1999 *Rev. Sci. Instrum*.**70**, 525.

Marshall F.J and O.Su. 1995 *Rev. Sci. Instrum* **66**, 725.

Missalla,T. et al.1999 *Rev. Sci. Instrum.*, **70**, 1288.

Miyanaga, M. et al.1983 *Appl. Phys. Lett.* **42**, 160

Murnane, M. M. et. al. 1991 Science **251**, 531

Perry,T.S. et al. 1991 *Phys.Rev. Lett*. **67**,3784

Pikuz, S.A. et al.1995 *JETP Lett.* **61**, 638 .

Pikuz, S.A. 1997 *Rev. Sci. Instr.* **68**, 740.

Pikuz, T.A. et al. 1995 *Journal of X-ray Science and Technology* **5**, 323 .

Rode, A.V. et al. 1990 *Opt. Commun*. **7**, 163.

Rosmej,F.B. et al.1997 *JQSRT* **58**, 859.
Sanchez del Rio, M. et al. 1995 *Rev. Sci. Instrum*. **66**, 5148.
Sanchez del Rio, M. et al. 1997 *Physica Scripta* **55**, 735.
Sancez del Rio, M. et al.1999 *Rev. Sci. Instrum*, **70**, 1614.
Stepanov, A.E. et al.1997 *JQSRT* **58**, 937.
Workman,J. et al.1999 *Rev. Sci. Instrum*.**70**, 613.

Fig 1

a)

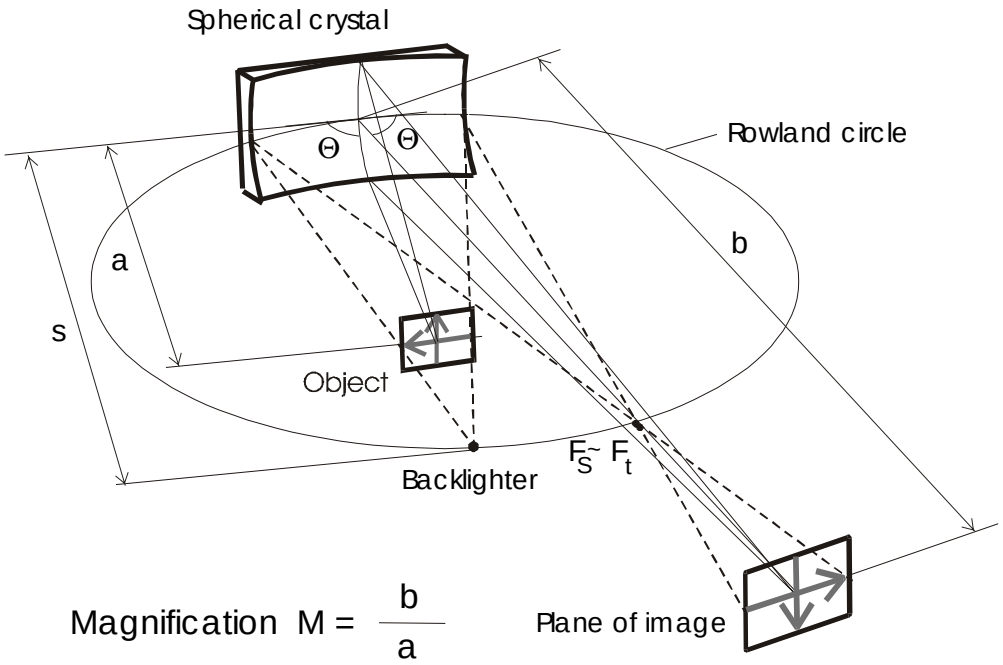

$$\text{Magnification } M = \frac{b}{a}$$

b)

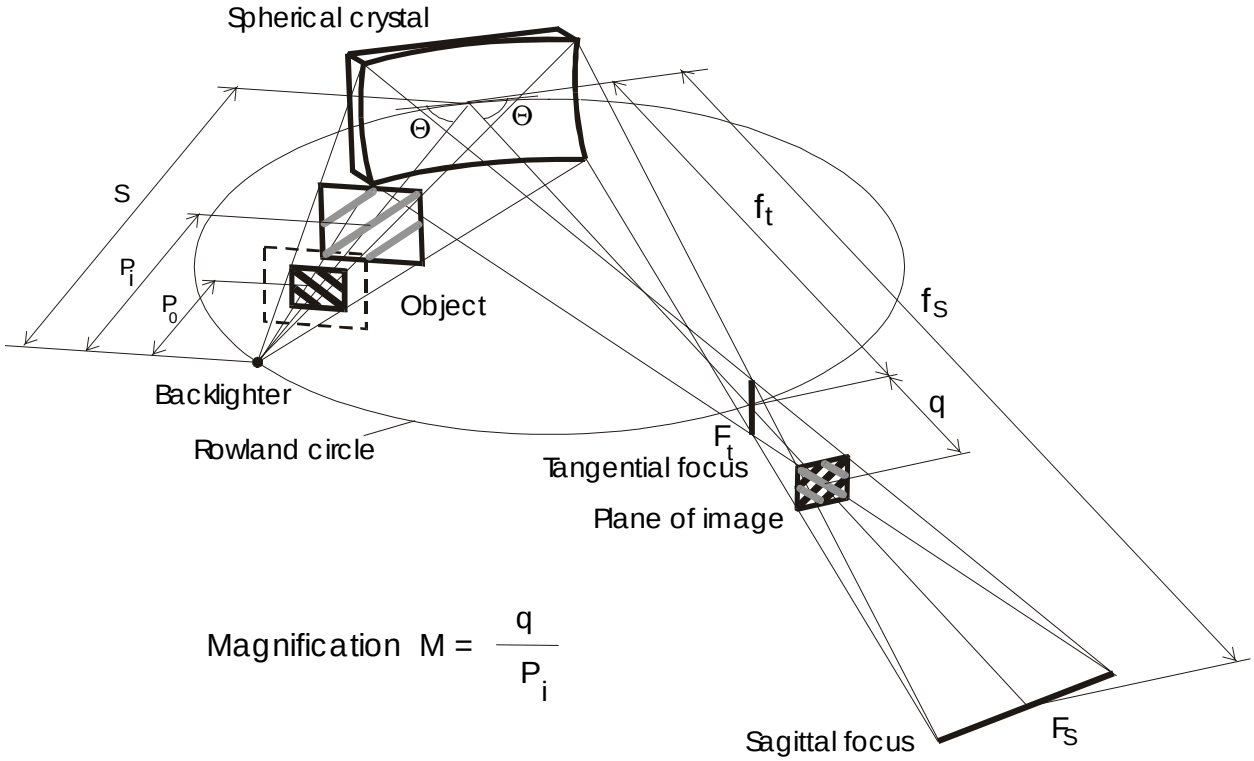

$$\text{Magnification } M = \frac{q}{P_i}$$

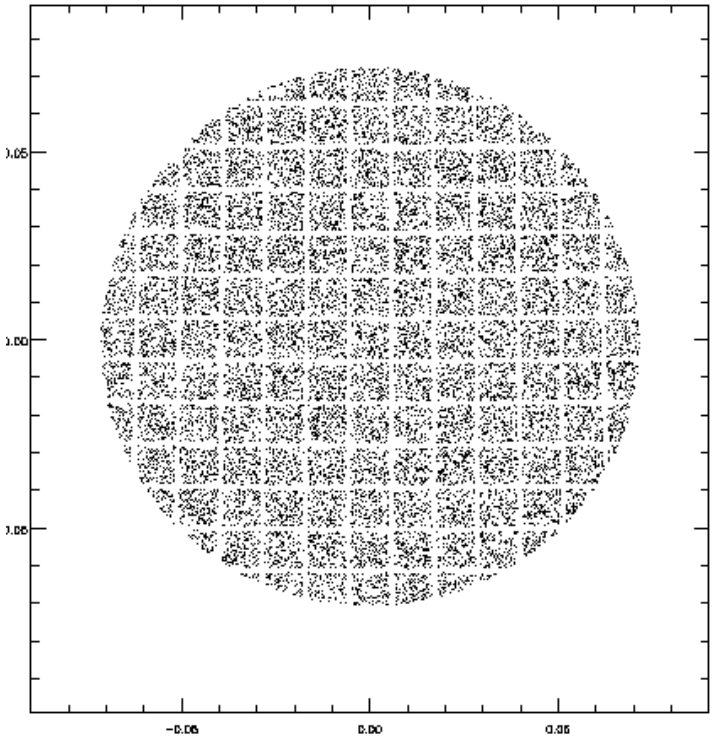

Fig 2a)

Fig 2b)

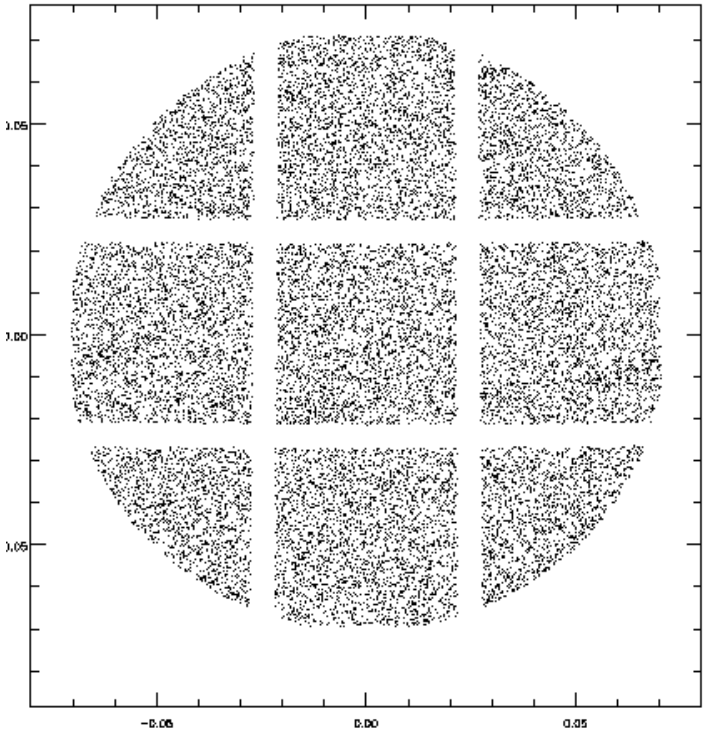

Fig3

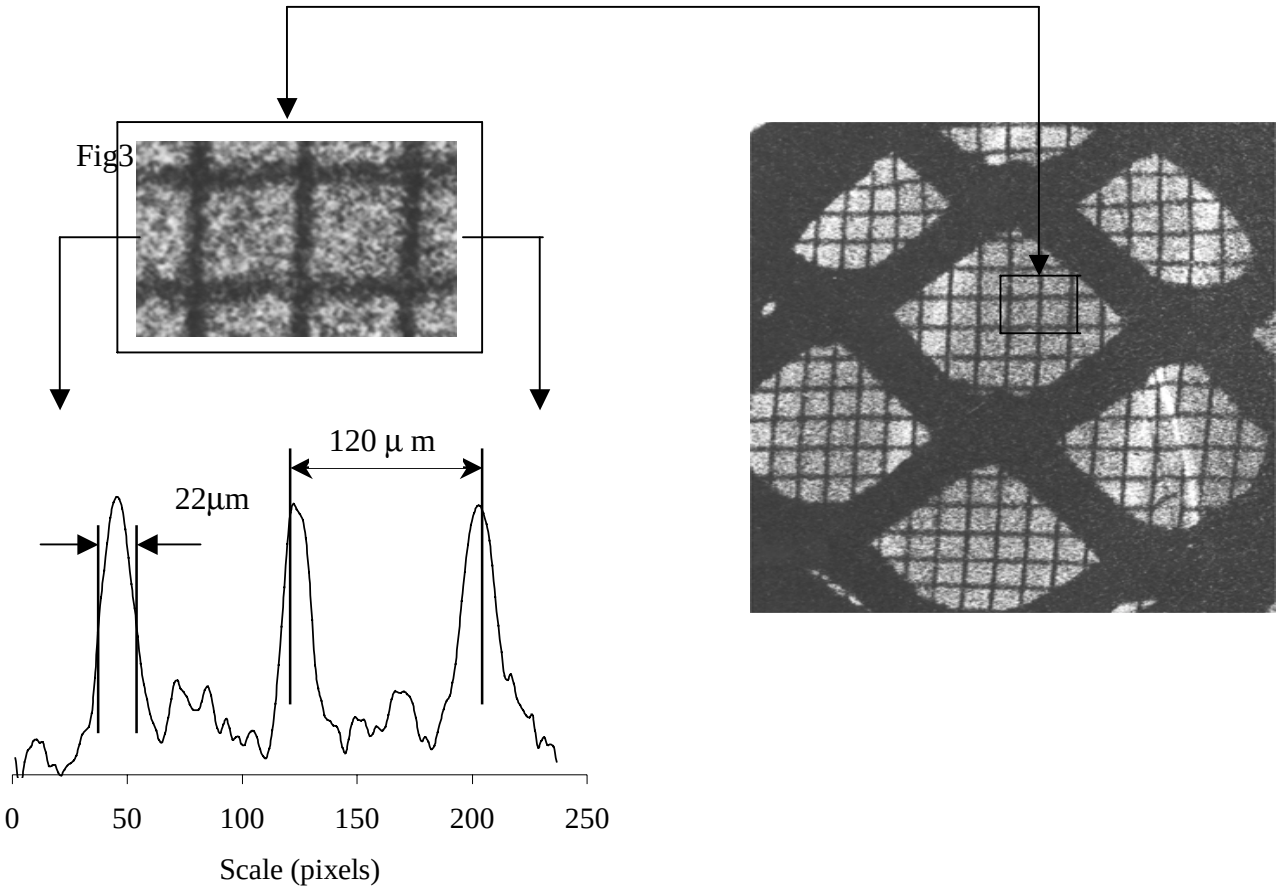

Fig 4

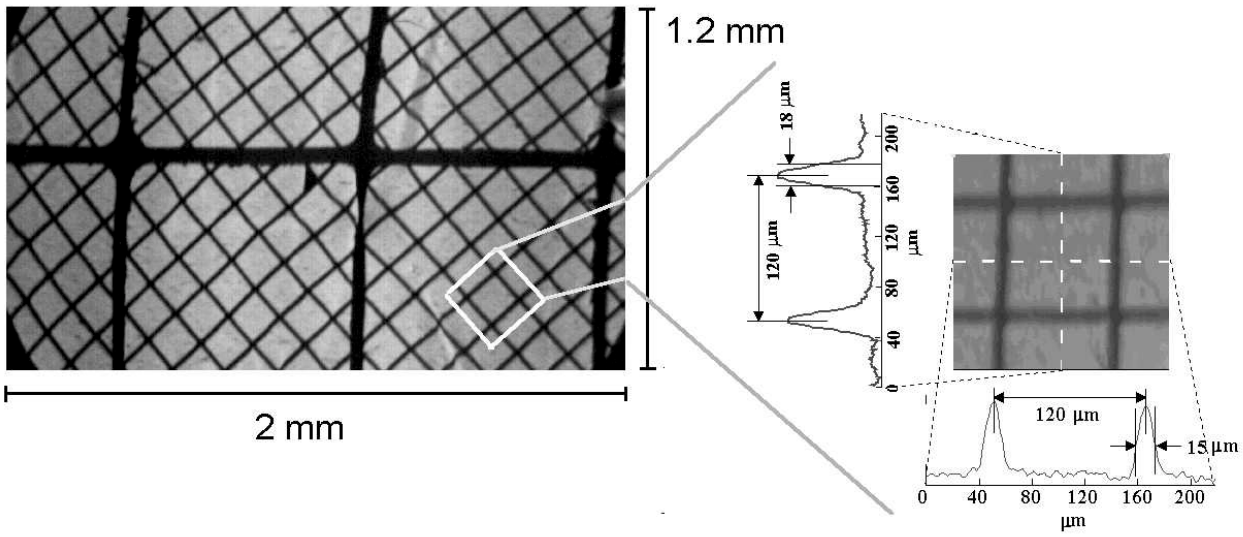
1.2 mm
2 mm
18 µm
120 µm
0
40
80
120
160
200
µm
120 µm
15 µm
0
40
80
120
160
200
µm

Fig 5

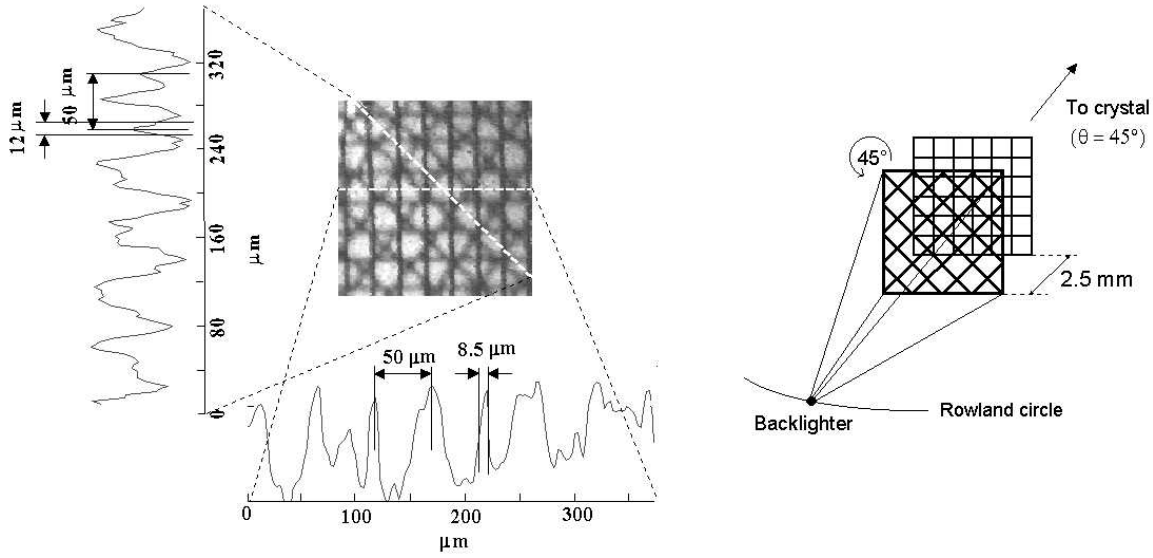
12 µm
50 µm
320
240
160
80
0
µm
50 µm
8.5 µm
0
100
200
300
µm
To crystal
(θ = 45°)
45°
2.5 mm
Backlighter
Rowland circle

Fig 6